Electrocatalytic Reduction of Dioxygen by Cobaltporphyrin in Aqueous Solutions

Seungwon Jeon*, Hyo Kyoung Lee, and Song Mi Kim

Department of Chemistry, Chonnam National University, Kwang-ju 500-757, Korea
Received February 14, 1998

The electrocatalytic reduction of dioxygen by $Co(TTFP)(Y)_2$ {Y=H_2O or HO^-} is investigated by cyclic voltammetry, spectroelectrochemistry, hydrodynamic voltammetry at a glassy carbon electrode in dioxygen-saturated aqueous solutions. Electrocatalytic reduction of dioxygen by $Co^{II}(TTFP)(Y)_2$ establishes a pathway of 2e reduction to form hydrogen peroxide, and then the generated hydrogen peroxide is reduced to water by $Co^{I}(TTFP)(Y)_2$ at more negative potential. $Co^{II}(TTFP)(Y)_2$ may bind dioxygen to produce the adduct complex [Co^{II}-O_2 or Co^{III}-$O_2^{\cdot-}$] which exhibits a Soret band at 411 nm and Q band at 531 nm.

Introduction

Electrocatalytic reduction of dioxygen has been receiving a great deal of attention for practical applications such as biological reactions, as well as fuel cells and air batteries over the past two decades.[1-33] Porphyrins or phthalocyanines of cobalt and iron are known as effective catalysts for dioxygen reduction. Many electrodes are chemically modified by the adsorption of several macromolecular compounds, which mediate the electron transfer. Dioxygen is reduced to hydrogen peroxide or water *via* 2e or 4e electron transfer at chemically modified electrodes. Among the various metalloporphyrins, the cobaltporphyrins have been well studied. It has previously been reported that water-soluble bisporphyrin structures act as effective catalysts for the 4e reduction of dioxygen to water in acidic solution at a pyrolytic graphite electrode.[25-31] Recently, it has been reported that monomeric cobaltporphyrins coordinated with some ruthenium complexes are useful as effective catalysts for the 4e reduction of dioxygen to water.[21-24] The electrocatalytic reduction of dioxygen has been studied using water-soluble iron, manganese, and cobalt tetra(4-*NN'N''*-trimethylanilinium) porphyrin (FeTMAP, MnTMAP, CoTMAP).[9-11] Dioxygen reduction proceeds *via* 4e electron transfer in acidic solutions in the presence of adsorbed or dissolved CoTMAP, but a major product at pH > 6 is HOOH by 2e electron transfer. In the present work, electrocatalytic reduction of dioxygen in dioxygen saturated aqueous solutions has been studied by cyclic voltammetry, spectroelectrochemistry, hydrodynamic voltammetry at a glassy carbon electrode using water-soluble cobalt tetra(1,2,5,6-tetrafluoro-4-*NN'N''*-trimethylanilinium) porphyrin [$Co(TTFP)(Y)_2$] (Figure 1). The electron withdrawing effects of phenyl substituents of $Co(TTFP)(Y)_2$ have been expected the positive shift of electrocatalytic potential for dioxygen reduction, but haven't been shown the potential shift. Although dioxygen is reduced to HOOH by acting of $Co^{II}(TTFP)(Y)_2$ as a catalyst, the generated HOOH is reduced to water by $Co^{I}(TTFP)(Y)_2$ in aqueous solutions. This study explores the use of Co^{I} porphyrin for the electrocatalytic reduction of HOOH. The electrochemical and spectroelectrochemical results will be discussed to determine the reduction pathway.

Experimental

The $CF_3SO_3^-$ salt of tetrakis-(1,2,5,6-tetrafluoro-4-*NN'N''*-trimethylanilinium) porphyrinato cobalt [Co(TTFP)], which is soluble in aqueous solutions in the entire pH range, was procured from Mid-Century Chemicals Co., USA. Sulfuric acid (Fischer scientific), potassium hydroxide (Alfa ultra pure), potassium nitrate (Wako pure), and buffer solutions (Fischer scientific) were used as received. All solutions for electrochemical and spectroelectrochemical experiments were prepared using doubly distilled deionized water.

The voltammetric measurements were accomplished with a three electrode potentiostat [Bioanalytical Systems (BAS) 100B/W]. A platinum-wire electrode separated from the analyte compartment by a medium porosity glass frit was used as an auxiliary electrode. A Ag/AgCl electrode supplied by BAS was used as a reference electrode, and the potential is approximately −45 mV relative to a saturated calomel electrode (SCE). A 3.0 mm diameter glassy carbon and 1.6 mm diameter platinum were employed as working electrodes for the redox reactions of cobaltporphyrin. All

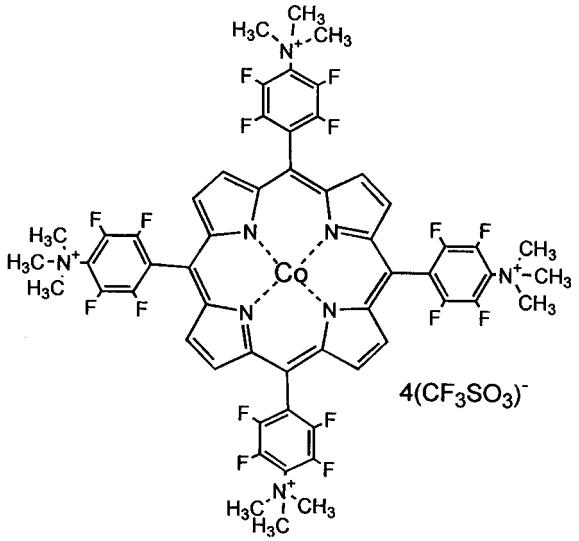

Figure 1. Structure of the water-soluble cobaltporphyrin employed in the present study.

working electrode surfaces were highly polished with alumina paste prior to each experiment. Spectroelectrochemical experiments were carried out in an optically transparent thin-layer cell containing a Pt mesh working electrode *via* controlled potential electrolysis using CV-27 potentiostat with three electrode system. Absorption spectra were recorded on a Jasco V-530 spectrophotometer equipped with an HMC-358 constant temperature cell holder, and an optical path length is 0.2 mm. Rotating disk experiments were conducted using a BAS RDE-1 instrument. Rotating ring-disk experiments were conducted using a AFRDE-5 instrument (Pine Instrument Company). A glassy carbon disk and a glassy carbon disk/platinum ring electrodes were used. The ring collection efficiency (N=0.17) was determined using a solution of ferrocene. Dioxygen concentrations in O_2-saturated solutions were used to be 1.2 mM at room temperature. All reported potentials were with respect to a Ag/AgCl electrode.

Results and Discussion

Electoreduction of $Co^{III}(TTFP)(Y)_2$ in the Absence of Dioxygen. Cyclic voltammograms (CVs) recorded with a glassy carbon electrode in a 0.5 mM $Co^{III}(TTFP)(Y)_2$ {Y=H_2O or HO^-} acidic solution are shown in Figure 2. $Co^{III}(TTFP)(Y)_2$ bears sixteen fluorides on the ortho and meta positions of phenyl group bonded to meso position of porphyrin ring and four positive charges on the trimethylanilinium entities (see Figure 1). There are three cathodic responses at +0.12, −0.32, and −0.76 V *vs.* Ag/AgCl for $Co^{III}(TTFP)(Y)_2$ dissolved in 0.1 N H_2SO_4 aqueous solution (Figure 2A and the solid line of Figure 2B), but CV of adsorbed $Co^{III}(TTFP)(Y)_2$ on the glassy carbon shows one cathodic peak at +0.13 V in 0.1 N H_2SO_4 solution (the dashed line of Figure 2B). When it is compared with CVs of dissolved and adsorbed $Co^{III}(TTFP)(Y)_2$, the peak near +0.12 V measured from dissolved $Co^{III}(TTFP)(Y)_2$ evidently arises from adsorbed $Co^{III}(TTFP)(Y)_2$. The peak at +0.12 V shown in the solid line of Figure 2B matchs +0.13 V peak obtained in the dashed line of Figure 2B. The peak at −0.32 V shown in the solid line of Figure 2B can be attributed to the reduction of $Co^{III}(TTFP)(Y)_2$ dissolved in 0.1 N H_2SO_4 solution because of the absence of its peak in the adsorbed $Co^{III}(TTFP)(Y)_2$. The large difference in the reduction potential between adsorbed and dissolved $Co^{III}(TTFP)(Y)_2$ indicates unusually favorable interactions between the electrode surface and the reduced cobalt center. The half-wave potential $E_{1/2}$ (+0.17 V) of first reduction for adsorbed $Co^{III}(TTFP)(Y)_2$ can be comparable to the $E_{1/2}$ (+0.18 V) of the first reduction for Co^{III}/Co^{II} couple of cobalt tetra(4-*NN'N''*-trimethylanilinium) porphyrin (CoTMAP) in 0.1 N H_2SO_4 solution.[9] The first reduction of dissolved $Co^{III}(TTFP)(Y)_2$ at −0.32 V is quasi-reversible and involves a one electron transfer. The reduction of $Co^{III}(TTFP)(Y)_2$ is established to be either metal or ligand centered. The first reduction of adsorbed and dissolved $Co^{III}(TTFP)(Y)_2$ may be metal centered and involves one electron process (discussed later). The second reduction of $Co^{III}(TTFP)(Y)_2$ in dissolved solution occurs at −0.76 V and its anodic couple at −0.69 V. The half-wave potential $E_{1/2}$ for the couple is −0.73 V, and the peak separation is 70 mV. The peak currents of the second reduction increase linearly with the square root of the scan rate, indicating a diffusion controlled process. The second reduction of $Co^{III}(TTFP)(Y)_2$ may also be metal centered and is one electron transfer reaction. There is no reduction peak at a potential near −0.76 V for adsorbed $Co^{III}(TTFP)(Y)_2$, indicating that the reduced form (Co^{II} porphyrin) may not be adsorbed on the glassy carbon electrode. The first reduction of $Co^{III}(TTFP)(Y)_2$ is poorly defined when compared with the second reduction of $Co^{III}(TTFP)(Y)_2$, and the current for the first reduction is lower than that for the second one. A similar decreased current of the Co^{III}/Co^{II} reaction has been reported for the redox of cobalt-porphyrins in DMF.[33] The lower current for the first reduction has been attributed to a slow rate-determining step in the electrochemical reaction between the six-coordinate Co^{III}

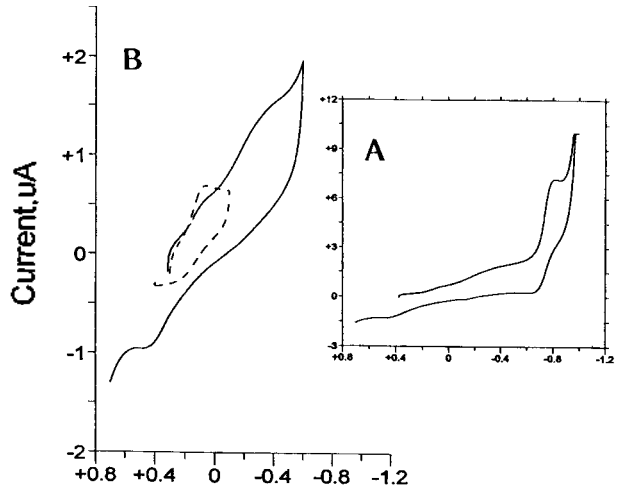

Figure 2. Cyclic voltammograms for the reduction of $Co^{III}(TTFP)(Y)_2$ in 0.1 N H_2SO_4 aqueous solution on the glassy carbon (50 mV/s scan rate). A: for dissolved 0.5 mM $Co^{III}(TTFP)(Y)_2$, B: for dissolved 0.5 mM $Co^{III}(TTFP)(Y)_2$ (solid line) and for adsorbed $Co^{III}(TTFP)(Y)_2$ (dashed line).

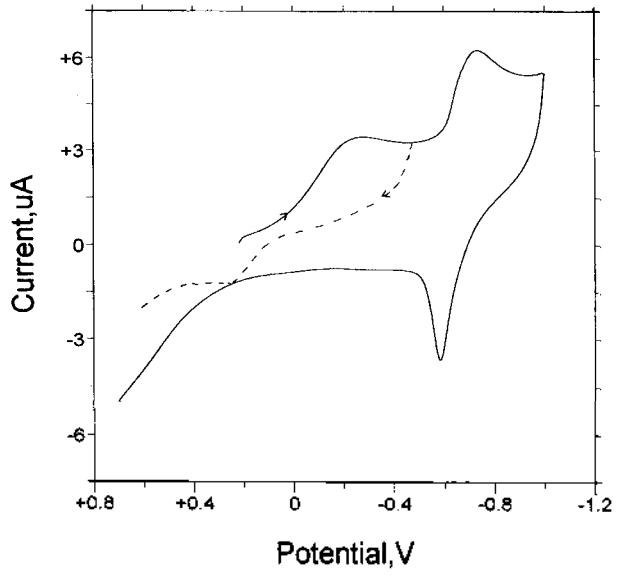

Figure 3. Cyclic voltammograms for 0.5 mM $Co^{III}(TTFP)(Y)_2$ at a glassy carbon electrode in a pH=7 buffer solution containing 0.2 N KNO_3 (50 mV/s scan rate).

and the five-coordinate Co^{II}.

Figure 3 illustrates cyclic voltammograms for $Co^{III}(TTFP)(Y)_2$ at a glassy carbon electrode in a pH=7 buffer solution containing 0.2 N KNO_3. There are two cathodic responses at −0.22 and −0.73 V for dissolved $Co^{III}(TTFP)(Y)_2$, but one reduction peak at near −0.22 V for adsorbed $Co^{III}(TTFP)(Y)_2$. The half-wave potentials for the reduction of $Co^{III}(TTFP)(Y)_2$ are +0.04 and −0.65 V, respectively. The peak currents of the first and second reductions increase linearly with the square root of the scan rate, indicating a diffusion controlled process. Based on the potential scan reversal in Figure 3, the reduced form $Co^{II}(TTFP)(Y)_2$ may be somewhat unstable under this condition.

Spectroelectrochemical Studies for $Co(TTFP)(Y)_2$ in Aqueous Solution. The electronic absorption spectra of Co^{III}, Co^{II}, and Co^{I} porphyrins were measured over the range of 350-600 nm by thin-layer spectroelectrochemical experiments. The successive spectra of $Co^{III}(TTFP)(Y)_2$ {Y= H_2O or HO^-} as observed during incremental reduction under argon atmosphere in a pH=7 buffer solution containing 0.2 N KNO_3 are exhibited in Figure 4. The spectrum of $Co^{III}(TTFP)(Y)_2$ shows a Soret band maximum at 421 nm and Q band at 536 nm. The spectrum of reduced form generated from the $1e^-$ reduction of $Co^{III}(TTFP)(Y)_2$ is obtained by holding the potential of the working electrode at −0.5 V. The optical spectra of the reduced form exhibits a Soret band maximum at 408 nm and Q bands at 524 and 556 nm. Examination of Figure 4 describes that the Soret band maximum at 421 nm diminishes and one at 408 nm appears. There are seen isosbestic points (414, 445 nm) which demonstrate the absence of any long-lived intermediates. No demetallation is observed as reported for $Co^{III}(TMAP)$.[9] On the basis of its Soret band, the absorbance at 408 nm is assigned to $Co^{II}(TTFP)(Y)_2$, this assignment is comparable to the results reported from the literature.[9,33] By the addition of dioxygen to $Co^{II}(TTFP)(Y)_2$, the electronic absorption spectrum exhibits a new Soret band maximum at 411 nm and Q band at 531 nm. The absorbance at 411 nm may be assigned to the adduct of Co(II)-dioxygen. These results indicate that Co^{II} porphyrin may bind dioxygen to produce the adduct complex [Co^{II}-O_2 or Co^{III}-O^{2-}].

The electronic absorption spectra of $Co^{I}(TTFP)(Y)_2$ and Co^{I}-dioxygen adduct obtained from thin-layer spectroelectrochemical experiments in a pH=7 buffer solution containing 0.2 N KNO_3 are illustrated in Figure 5. The spectrum of reduced form generated from the 2e⁻ reduction of $Co^{III}(TTFP)(Y)_2$ is obtained by holding the potential of the working electrode at −0.9 V. The spectrum of the product obtained from the 2e⁻ reduction of $Co^{III}(TTFP)(Y)_2$ exhibits a Soret band maximum at 414 nm and Q band at 533 nm (b of Figure 5), and the absorbance at 414 nm is assigned to $Co^{I}(TTFP)(Y)_2$. Likewise, the addition of dioxygen to $Co^{I}(TTFP)(Y)_2$ results in the spectrum of Co(I)-dioxygen adduct giving a Soret band maximum at 424 nm and Q band at 543 nm (c of Figure 5).

Electocatalytic Reduction of Dioxygen by Co(TTFP)(Y)$_2$. The presence of $Co^{III}(TTFP)(Y)_2$ in 0.1 N H_2SO_4 solution results in a positive shift of the reduction potential for dioxygen reduction and this process occurs at E_{pc} =+0.10 V. The reduction potential of dioxygen in the presence of $Co^{III}(TTFP)(Y)_2$ is nearly 0.7 V positive shift compared to the potential in the absence of $Co^{III}(TTFP)(Y)_2$ at a given scan rate (50 mV/s). The effect of scan rate on the peak current for the reduction of dioxygen in the presence of $Co^{III}(TTFP)(Y)_2$ is shown in Figure 6. The linearity of

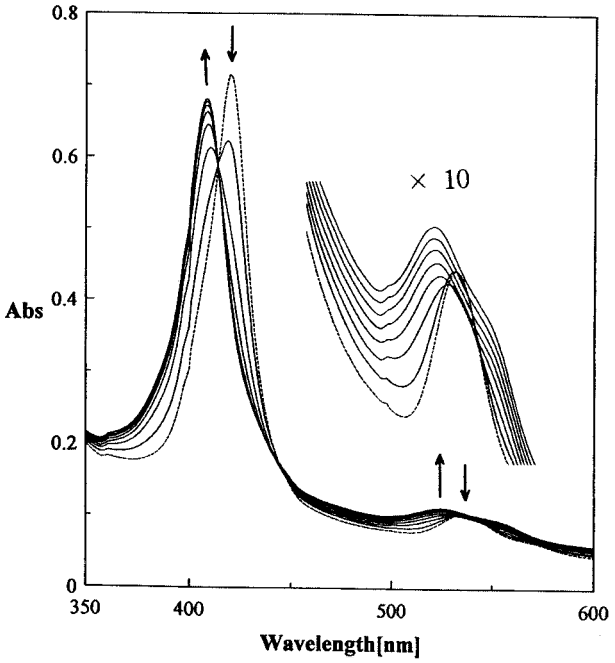

Figure 4. The electronic absorption spectra obtained during incremental reduction at −0.5 V of a deaerated pH=7 buffer solution containing 0.2 N KNO_3 containing 0.2 mM $Co^{III}(TTFP)(Y)_2$. The arrows indicates the direction of the absorbance change during reduction.

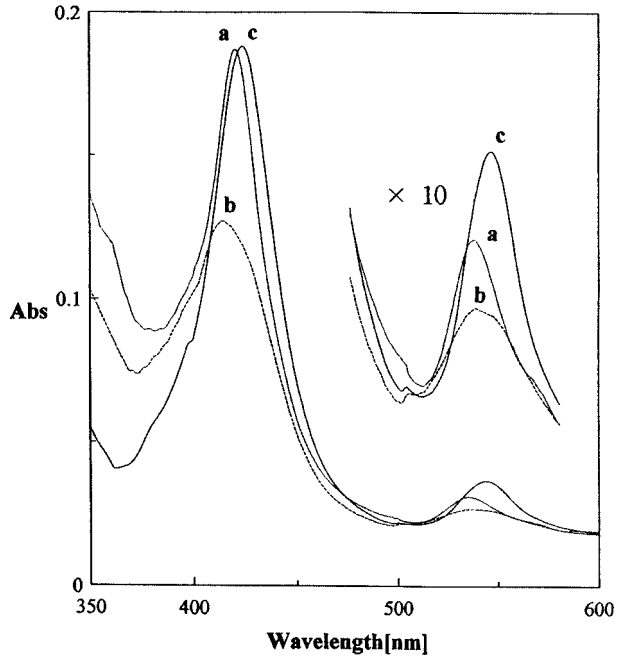

Figure 5. The electronic spectrum obtained from 2e⁻ reduction of 0.2 mM $Co^{III}(TTFP)(Y)_2$ in a deaerated pH=7 buffer solution containing 0.2 N KNO_3 (b), after the addition of dioxygen to reduced cobalt species (c). (a) represents a starting species.

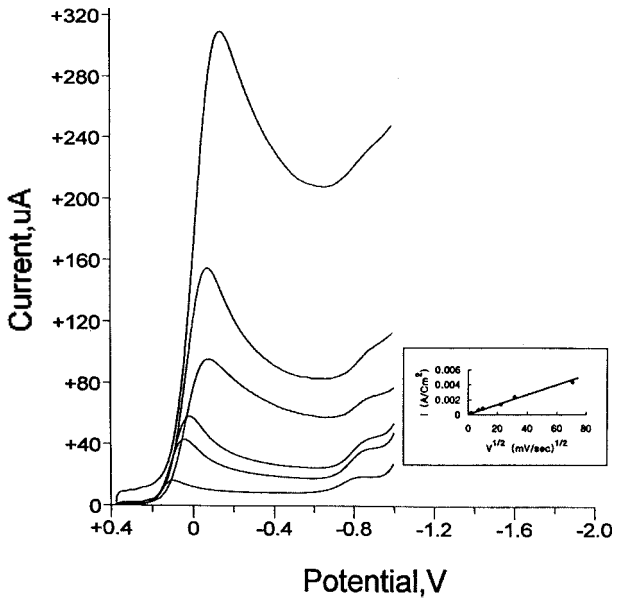

Figure 6. Cyclic voltammograms for the reduction of dioxygen in the presence of $Co^{III}(TTFP)(Y)_2$ in 0.1 N H_2SO_4 solution at different scan rates on a glassy carbon electrode. The inside plot represents the analysis of first peak current *vs.* (scan rate)$^{1/2}$ for the electroreduction of dioxygen, $[O_2]$=1.2 mM.

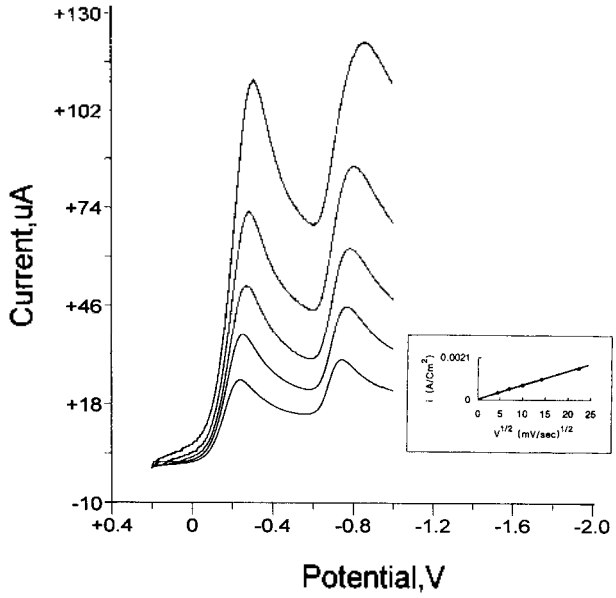

Figure 7. Cyclic voltammograms for the reduction of dioxygen in the presence of $Co^{III}(TTFP)(Y)_2$ in a pH=7 buffer solution containing 0.2 N KNO_3 at different scan rates on a glassy carbon electrode. The inside plot represents the analysis of first peak current *vs.* (scan rate)$^{1/2}$ for the electroreduction of dioxygen.

the peak current *vs.* the square root of the scan rate plot indicates that electrocatalytic reduction of dioxygen is a diffusion controlled process when the dioxygen concentration is held constant (inside Figure 6). The first reduction process corresponding to the Co^{III}/Co^{II} couple upon adsorption of $Co^{III}(TTFP)(Y)_2$ on the glassy carbon electrode surface is located at E_{pc}=+0.12 V at 50 mV/s, and the electrocatalytic reduction peak potential of dioxygen is +0.10 V at same scan rate. The dioxygen reduction by $Co^{II}(TTFP)(Y)_2$ generated from the $1e^-$ reduction of $Co^{III}(TTFP)(Y)_2$ results in the formation of HOOH by two-electron process. Examination of Figure 6 describes that HOOH formed from dioxygen reduction is also reduced electrocatalytically at near −0.76 V where $Co^{II}(TTFP)(Y)_2$ is reduced to $Co^{I}(TTFP)(Y)_2$, and the cathodic current decreases with an increase of scan rate, indicating that the electroreduction rate of HOOH by $Co^{I}(TTFP)(Y)_2$ may be slow. It is well known that Co^{II} porphyrin does not act as a catalyst for the reduction of HOOH,[34] but there is no report for the effect of Co^{I} porphyrin as a catalyst for the reduction of HOOH. Co^{I} porphyrin can catalyze the electroreduction or disproportionation of HOOH. The separate experiments confirm that the electroreduction of HOOH by $Co^{I}(TTFP)(Y)_2$ occurs under the same conditions, and that the disproportionation of HOOH by Co^{I} porphyrin is very slow. It can be concluded that the reduced form $Co^{I}(TTFP)(Y)_2$ can act as a catalyst for the reduction of HOOH.

Meanwhile, Figure 7 illustrates the effect of scan rate on the peak current for the reduction of dioxygen in the presence of $Co^{III}(TTFP)(Y)_2$ in a pH=7 buffer solution containing 0.2 N KNO_3. The first reduction process corresponding to the Co^{III}/Co^{II} transition is located at E_{pc}= − 0.22 V at 50 mV/s, and the electroreduction peak potential of dioxygen is − 0.25 V. The peak currents for dioxygen reduction increase linearly with the square root of the scan rate, indicating a diffusion controlled process (inside Figure 7). Based on these observations in any solutions employed it is suggested that $Co^{II}(TTFP)(Y)_2$ is an active species in the electrocatalytic reduction of dioxygen, and $Co^{I}(TTFP)(Y)_2$ is an effective catalyst for the electroreduction of HOOH which is formed from dioxygen reduction. The electroreduc-

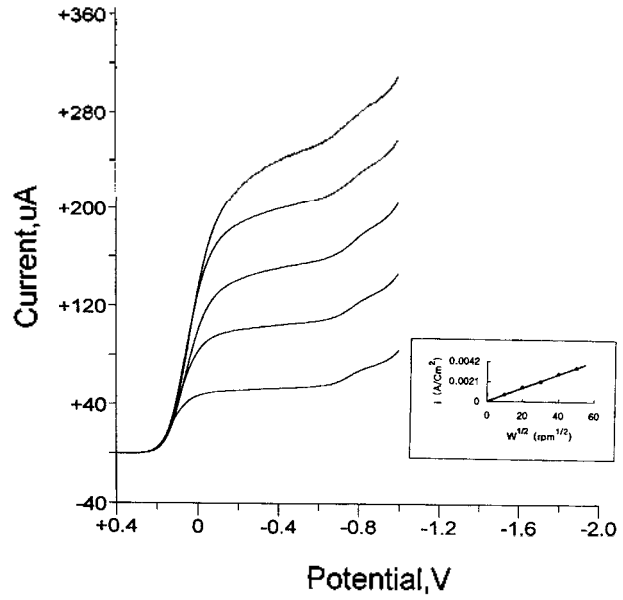

Figure 8. RDE voltammograms of dioxygen reduction for an dioxygen-saturated solution of $Co^{III}(TTFP)(Y)_2$ in 0.1 N H_2SO_4 solution at 10 mV/s scan rate on a glassy carbon disk. The inside plot represents Levich plot of plateau current (at − 0.5 V) *vs.* (rotation rate)$^{1/2}$ for the voltammograms.

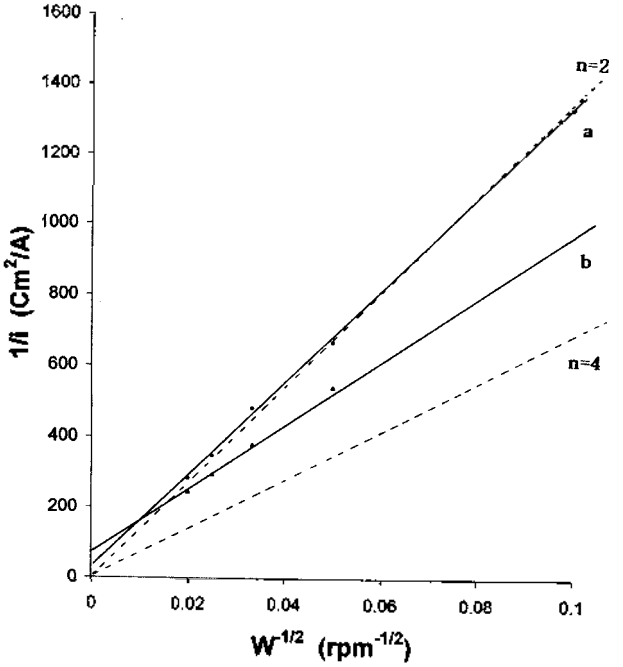

Figure 9. Koutecky-Levich plots for dioxygen reduction catalyzed by $Co^{III}(TTFP)(Y)_2$ in 0.1 N H_2SO_4 solution at 10 mV/s scan rate on a glassy carbon disk. The dashed lines were calculated for the diffusion-convection limited reduction by two and four electrons, respectively. (a) obtained from the first plateau current measured near − 0.5 V, (b) obtained from the second plateau current measured near − 0.9 V.

tion potential of dioxygen coincides with the reduction potential of $Co^{III}(TTFP)(Y)_2$ over the pH range employed. This coincidence indicates that the potential governing dioxygen reduction is the reduction potential of $Co^{III}(TTFP)(Y)_2$ to $Co^{II}(TTFP)(Y)_2$, this is consistent with an EC mechanism which has been proposed for other water-soluble metalloporphyrins. Likewise, the electroreduction potential of HOOH coincides with the reduction potential of $Co^{II}(TTFP)(Y)_2$ over the given pH range, indicating that the potential governing HOOH reduction is also the reduction potential of $Co^{II}(TTFP)(Y)_2$ to $Co^{I}(TTFP)(Y)_2$.

Further investigations carried out using hydrodynamic voltammetry {rotating disk electrode (RDE) and rotating ring-disk electrode (RRDE)} confirm the formation of hydrogen peroxide as a major product of dioxygen reduction by reduced form $Co^{II}(TTFP)(Y)_2$. The glassy carbon disk potential is scanned from +0.6 V to − 1.0 V at a scan rate of 10 mV/s in dioxygen-saturated 0.1 N H_2SO_4 solution. RDE voltammograms obtained from the dissolved solution of $Co^{III}(TTFP)(Y)_2$ are shown in Figure 8. A Levich plot of the disk limiting current against the square root of rotation rate is linear (inside Figure 8), indicating the occurrence of a diffusion controlled reaction. Koutecky-Levich plots for dioxygen reduction catalyzed by $Co^{II}(TTFP)(Y)_2$ are shown in Figure 9. The dashed lines were calculated for the diffusion-convection limited reduction by two and four electrons, respectively. Two solid lines are obtained from the first plateau current measured near − 0.5 V (a), and the second plateau current measured near − 0.9 V (b). The number of electrons transferred estimated from the slope of the Koutecky-

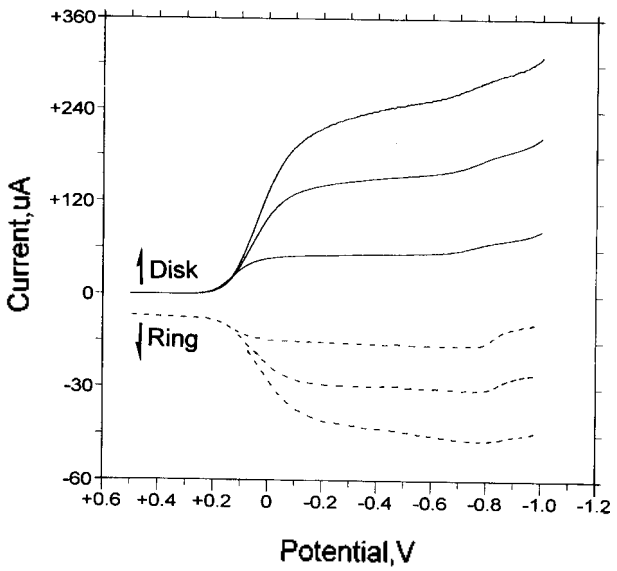

Figure 10. RRDE voltammograms (E^r=+1.0 V) of dioxygen reduction for an dioxygen-saturated solution of $Co^{III}(TTFP)(Y)_2$ in 0.1 N H_2SO_4 solution at 10 mV/s scan rate, the rotation rates are 100, 900, and 2500 rpm.

Levich plot reveals that the dioxygen reduction by $Co^{II}(TTFP)(Y)_2$ occurs in two-electron process (a of Figure 9), and the total electron for successive dioxygen reduction by Co^{II} and Co^{I} is about four (b of Figure 9). On the basis of these results, it can be concluded that limiting current obtained from the first plateau results from the electrocatalytic reduction of dioxygen to HOOH by acting of $Co^{II}(TTFP)(Y)_2$ as a catalyst, and then limiting current obtained from the second plateau may be related to the electroreduction of HOOH to water by the $Co^{I}(TTFP)(Y)_2$ complex as a catalyst.

Typical RRDE voltammograms obtained in a dioxygen-saturated 0.1 N H_2SO_4 solution and in the presence of $Co^{III}(TTFP)(Y)_2$ are exhibited in Figure 10. The disk potential is scanned from +0.6 V to − 1.0 V at a scan rate of 10 mV/s while the potential of the ring electrode is maintained at +1.0 V. Ring currents corresponding to the formation of HOOH have been observed under these conditions. The result indicates that the major product of dioxygen reduction by $Co^{II}(TTFP)(Y)_2$ is HOOH, and then HOOH as an initial product may be reduced to water by an effective catalyst of $Co^{I}(TTFP)(Y)_2$ near − 0.9 V potential when judged from the decrease of HOOH formation near − 0.9 V.

Acknowledgment. This paper was supported by Non Directed Research Fund, Korea Research Foundation, 1996.

References

1. Yeager, B.; Franklin, A. D., Ed. *Electrocatalysis on Non-Metallic Surfaces*; N.B.S. Special Publication No. 455, 1976, 203.
2. Yeager, E.; Zagal, J.; Nikovic, B. Z.; Adzic, R. R. In *Proceedings of the Third Symposium on Electrode Processes. The Electrochem. Soc.* **1979**, 436.
3. Bettelheim, A.; Chan, R.; Kuwana, T. *J. Electroanal. Soc.* **1979**, *99*, 391.
4. Bettelheim, A.; Chan, R.; Kuwana, T. *J. Electroanal. Chem.* **1980**, *110*, 93.

5. Forshey, P. A.; Kuwana, T. *Inorg. Chem.* **1981**, *19*, 693.
6. Forshey, P. A.; Kuwana, T.; Kobayashi, N.; Osa, T. *Adv. Chem. Ser.* **1982**, *201*, 601.
7. Kuwana, T.; Fujihira, M.; Sunakawa, K.; Osa, T. *J. Electroanal. Chem.* **1978**, *88*, 299.
8. Ozer, D.; Harth, R.; Mor, U.; Bettelheim, A. *J. Electroanal. Chem.* **1989**, *266*, 109.
9. Ozer, D.; Parash, R.; Broitman, F.; Mor, V.; Bettelheim, A. *J. Chem. Soc., Faraday Trans. I* **1984**, *80*, 1139.
10. Bettelheim, A.; Parash, R.; Ozer, D. *J. Electrochem. Soc.* **1982**, *129*, 2247.
11. Bettelheim, A.; Ozer, D.; Parash, R. *J. Chem. Soc., Faraday Trans. I* **1983**, *79*, 1555.
12. Creager, S. E.; Raybuck, S. A.; Murray, R. W. *J. Am. Chem. Soc.* **1986**, *108*, 4225.
13. Creager, S. E.; Murray, R. W. *Inorg. Chem.* **1987**, *26*, 2612.
14. Perree-Fauvet, M.; Gandemer, A.; Bonvoison, J.; Girerd, J. J.; Boucly-Goester, C.; Boucly, P. *Inorg. Chem.* **1989**, *28*, 3533.
15. Tsang, P. K. S.; Sawyer, D. T. *Inorg. Chem.* **1990**, *29*, 2848.
16. Sazou, D.; Araullo-McAdams, C.; Han, B. C.; Franzen, M. M.; Kadish, K. M. *J. Am. Chem. Soc.* **1990**, *112*, 7879.
17. D'Souza, F.; Deviprasad, G. R.; Hsieh, Y.-Y. *J. Electroanal. Chem.* **1996**, *411*, 167.
18. Shigehara, K.; Anson, F. C. *J. Phys. Chem.* **1982**, *86*, 2776.
19. Ni, C. L.; Anson, F. C. *Inorg. Chem.* **1985**, *24*, 4754.
20. Durand, R. R.; Anson, F. C. *J. Electroanal. Chem.* **1982**, *134*, 273.
21. Shi, C.; Anson, F. C. *J. Am. Chem. Soc.* **1991**, *113*, 9564.
22. Shi, C.; Anson, F. C. *Inorg. Chem.* **1995**, *34*, 4554.
23. Steiger, B.; Anson, F. C. *Inorg. Chem.* **1994**, *33*, 5767.
24. Steiger, B.; Anson, F. C. *Inorg. Chem.* **1995**, *34*, 3355.
25. Collman, J. P.; Chang, L. L.; Tyvoll, D. A. *Inorg. Chem.* **1995**, *34*, 1311.
26. Collman, J. P.; Wagenknecht, P. S.; Hutchison, J. E. *Angew. Chem., Int. Ed. Engl.* **1994**, *33*, 1537.
27. Collman, J. P.; Denisevich, P.; Kanai, Y.; Marrocco, M.; Koval, C.; Anson, F. C. *J. Am. Chem. Soc.* **1980**, *102*, 6027.
28. Chang, C. K.; Liu, H. Y.; Abdalmuhdi, I. *J. Am. Chem. Soc.* **1984**, *106*, 2726.
29. Karaman, R.; Jeon, S.; Almarsson, O.; Blasko, A.; Bruice, T. C. *J. Am. Chem. Soc.* **1992**, *114*, 4899.
30. Jeon, S.; Almarsson, O.; Karaman, R.; Blasko, A.; Bruice, T. C. *Inorg. Chem.* **1993**, *32*, 2562.
31. Choi, Y-K.; Jeon, S.; Park, J-K.; Chjo, K-H. *Electrochim. Acta* **1997**, *42*, 1287.
32. Battersby, A. R.; Fookes, C. J. R.; Matcham, C. W. J.; McDonald, E. *Nature (London).* **1980**, *285*, 17.
33. Lin, X. Q.; B.-Cocolios, B.; Kadish, K. M. *Inorg. Chem.* **1986**, *25*, 3242.
34. Chan, R.; Su, Y. O.; Kuwana, T. *Inorg. Chem.* **1985**, *24*, 3777.

Real Time Monitoring of Ionic Species Generated from Laser-Ablated $Pb(Zr_{0.52}Ti_{0.48})O_3$ Target Using Pulsed-Field Time-Of-Flight Mass Spectrometer

Young-Ku Choi, Hoong-Sun Im†, and Kwang-Woo Jung*

Department of Chemistry, Wonkwang University, Iksan 570-749, Korea
†Korea Research Institute of Standards and Science, Taeduk Science Town, Taejon 305-600, Korea
Received February 20, 1998

The characteristics of the ablation plume generated by 532 nm Nd:YAG laser irradiation of a $Pb(Zr_{0.52}Ti_{0.48})O_3$ (PZT) target have been investigated using a pulsed-field time-of-flight mass spectrometer (TOFMS). The relative abundance of O^+, Ti^+, Zr^+, Pb^+, TiO^+, and ZrO^+ ions has been measured and discussed. TiO^+ and ZrO^+ ions were also found to be particularly stable within the laser ablation plasma with respect to PbO^+ species. The behavior of the temporal distributions of each ionic species was studied as a function of the delay time between the laser shot and the ion extraction pulse. The most probable velocity of each ablated ion is estimated to be V_{mp}=1.1-1.6$\times 10^5$ cm/s at a laser fluence of 1.2 J/cm^2, which is typically employed for the thin film deposition of PZT. The TOF distribution of Ti^+ and Zr^+ ions shows a trimodal distribution with one fast and two slow velocity components. The fast velocity component (6.8×10^5 cm/s) appears to consist of directly ablated species via nonthermal process. The second component, originated from the thermal evaporation process, has a characteristic velocity of 1.4-1.6$\times 10^5$ cm/s. The slowest component (1.2×10^5 cm/s) is composed of a dissociation product formed from the corresponding oxide ion.

Introduction

Lead zirconate titanate, $Pb(Zr_xTi_{1-x})O_3$ (PZT), has attracted much attention due to the promise of applications in devices such as non-volatile random access memories,[1] electro-optic switches,[2] pyroelectric sensors,[3] and piezoelectric surface and bulk wave transducers.[4-6] Pulsed laser deposition (PLD) has become a powerful and efficient tech-

*Author to whom correspondence should be addressed.